Bioorganic & Medicinal Chemistry Letters 19 (2009) 469–473

Contents lists available at ScienceDirect

Bioorganic & Medicinal Chemistry Letters

journal homepage: www.elsevier.com/locate/bmcl

Discovery of 4,6-bis-anilino-1*H*-pyrrolo[2,3-*d*]pyrimidines: Potent inhibitors of the IGF-1R receptor tyrosine kinase

Stanley D. Chamberlain [a], Joseph W. Wilson [a], Felix Deanda [b], Samarjit Patnaik [a], Anikó M. Redman [a], Bin Yang [a], Lisa Shewchuk [b], Peter Sabbatini [c], M. Anthony Leesnitzer [d], Arthur Groy [c], Charity Atkins [c], Roseanne Gerding [a], Anne M. Hassell [b], Huangshu Lei [a], Robert A. Mook Jr. [a], Ganesh Moorthy [c], Jason L. Rowand [c], Kirk L. Stevens [a], Rakesh Kumar [c], J. Brad Shotwell [a,*]

[a] GlaxoSmithKline, Oncology R&D, 5 Moore Drive, 3.4184.4B, PO Box 13398, Research Triangle Park, NC 27709-3398, USA
[b] GlaxoSmithKline, Computational and Structural Chemistry, 5 Moore Drive, Research Triangle Park, NC 27709, USA
[c] GlaxoSmithKline, Oncology R&D, 1250 S. Collegeville Road, Collegeville, PA 19426, USA
[d] GlaxoSmithKline, Molecular Discovery Research, 5 Moore Drive, Research Triangle Park, NC 27709, USA

ARTICLE INFO

Article history:
Received 8 October 2008
Revised 8 November 2008
Accepted 12 November 2008
Available online 18 November 2008

Keywords:
Pyrrolopyrimidine
IGF-1R
Kinase inhibitor
IGF-IR

ABSTRACT

The evaluation of a series of 4,6-bis-anilino-1*H*-pyrrolo[2,3-*d*]pyrimidines as inhibitors of the IGF-1R (IGF-IR) receptor tyrosine kinase is reported. Examples demonstrate nanomolar potencies in in vitro enzyme and mechanistic cellular assays as well as promising in vivo pharmacokinetics in rat.

The IGF-1R signaling pathway is activated in many human cancers including prostate,[1] colon,[2] breast,[3] and pancreas[4] by overexpression of IGF-1R or its ligands IGF-1 and 2 and/or by decreased levels of IGF binding proteins. Inhibition of IGF-1R signaling using a variety of approaches (e.g., anti-IGF-1R antibodies, antisense, IGF binding proteins, siRNA) has resulted in decreased proliferation and survival of tumor cells in vitro and in vivo.[5] Further, IGF-1R activation has been associated with resistance to targeted agents such as trastuzumab[6] in breast cancer. Therefore, inhibition of IGF-1R signaling may reverse resistance to targeted agents under certain conditions. These observations have led to the development of a number of potent small-molecule inhibitors of IGF-1R in diverse chemical space.[7] We report herein the investigation of a series of 4,6-bis-anilino-1*H*-pyrrolo[2,3-*d*]pyrimidines, whose syntheses have been described elsewhere,[8] as potent inhibitors of the IGF-1R receptor tyrosine kinase.

Pyrrolopyrimidine **1** was identified from a focused library consisting of small molecules with known kinase inhibitory motifs. A remarkable kinase selectivity profile was observed for **1**, wherein 48 of 52 kinases screened in the initial panel showed IC_{50} values of >100 nM (50-fold selectivity relative to IGF-1R). However, in addition to IGF-1R, pyrrolopyrimidine **1** also potently inhibited JNK1, ALK, and IR, with IC_{50}s of 12, 1.0, and 6.3 nM, respectively.

Figure 1. Model of IGF-1R (carbon atoms in grey) in complex with **1** (carbon atoms in green). Intermolecular H-bond interactions are highlighted with yellow lines.

* Corresponding author.
E-mail address: JBS26900@GSK.com (J.B. Shotwell).

0960-894X/$ - see front matter © 2008 Elsevier Ltd. All rights reserved.
doi:10.1016/j.bmcl.2008.11.046

To provide a structure-based rationale for medicinal chemistry efforts, a docking model of the IGF-1R kinase domain in complex with **1** was constructed using available crystallographic data (Fig. 1).[9] Lead **1** forms three H-bond interactions at the hinge region, one with the backbone carbonyl of Glu1050 and the second with the backbone amino group of Met1052. A third H-bond is also highlighted between the C6 amino group and the backbone carbonyl of Met1052. The 2-aminobenzamide occupies the inner hydrophobic region of the ATP-binding site with the phenyl making van der Waals contact with Leu975, Gly976, Gln977 and Val983. The carboxamide is directed toward Lys1003 (catalytic lysine) and Asp1123 (of the DFG motif), but does not form an H-bond interaction with either residue. Instead, the carboxamide forms an intramolecular H-bond with the C4 amino group forming a pseudo-six membered ring. The C6 aniline occupies the outer hydrophobic region of the pocket where it makes van der Waals contact with Leu975, Gly1055 and Met1112. The C2′ methyl is directed toward the hinge region where it interacts with Leu975, Leu1051 and Thr1053. Lastly, the 1-propyl-tetrahydro-3-pyridinyl lies outside the pocket and is thus solvent exposed.

Initial structural optimizations were focused on the C6 aniline, wherein it was anticipated substitution at C2′ in particular would be crucial for efficient binding to IGF-1R because of both spatial proximity to Leu1051 and influence on the C6 aniline N–H pK_a. As illustrated in Table 1, a C2′ methoxy substituent proved optimal (see **5** and **6**). Bulkier alkoxy substituents (**7**) and strong electron withdrawing substituents (**4**) were less potent in screening at both the enzyme[10] and cellular[11] level (Table 1). Smaller substituents (**2** and **3**) gave reasonable enzyme potency but suffered from a reduced kinase selectivity profile.[12] Simple fluorination at R^4 (i.e., **5** vs **6**) had only minimal influence on inhibitor potency, but proved important in reducing in vivo metabolism (vida infra).

Consistent with the model, tolerability to a wide variety of substituents was anticipated at C4′ because of its orientation toward solvent (Fig. 1), and removal of the unsaturated piperidine was desirable from a safety perspective.[13] Indeed, both saturated 3- and 4-substituted piperidines (Table 1, **8** and **9**) and 1,4-disubstituted piperazines (Table 1, **10** and **11**) possess excellent potency against IGF-1R. Additionally, the distal latent amine was not required, as morpholine-substituted **12** proved to be an exceptionally potent inhibitor of IGF-1R. Initially, synthetic tractability and promising pharmacokinetic properties (vida infra) led us to explore the piperazine subseries exemplified by **10** and **11** more carefully.

Crystallographic confirmation of the binding mode for the pyrrolopyrimidine series of IGF-1R inhibitors was achieved through the use of an IR double mutant (C981S, D1132N). Given that the sequence identity between IGF-1R and IR is roughly 85% over their kinase binding domains and identical within the ATP-binding cleft, IR was a reasonable surrogate for IGF-1R. A co-crystal structure of our IR mutant in complex with **13** was produced and is illustrated in Figure 2. The overall binding mode for **13** was similar to that modeled for **1** in complex with IGF-1R. Key intermolecular interactions included the H-bonding of **13** to IR at the hinge region via the inhibitor's pyrrolopyrimidine. Also, as with our docking model, the H-bond interaction between the C6 amino group and the backbone carbonyl of Met1079 was at a non-ideal angle and distance. Interestingly, the carboxamide did interact indirectly with Asp1150 through a water-mediated interaction. Finally, the C2′ methoxy was directed towards the hinge region in similar fashion to the C2′ methyl of **1**, while

Table 1
IGF-1R enzyme IC_{50} and phospho IGF-1R cellular IC_{50} results for **1–12**. (values represent an average of ⩾2 individual measurements)

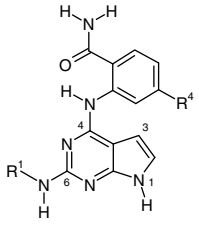

Compound	R^4	R^1	X	IGF-1R Enzyme IC_{50} (nM)	Phospho IGF-1R Cellular IC_{50} (nM)
1	H		–Me	5.0	—
2	H		–H	1.6	—
3	H		–F	1.6	317
4	H		$-CF_3$	20	>10,000
5	H		–OMe	0.6	104
6	F		–OMe	0.8	82
7	F		–O*i*Pr	3.2	2240
±8	F		–Pr	0.4	60
9	F		–Pr	0.3	47
10	F		–Pr	1.6	122
11	F		–*i*Pr	0.8	130
12	F		—	1.6	68

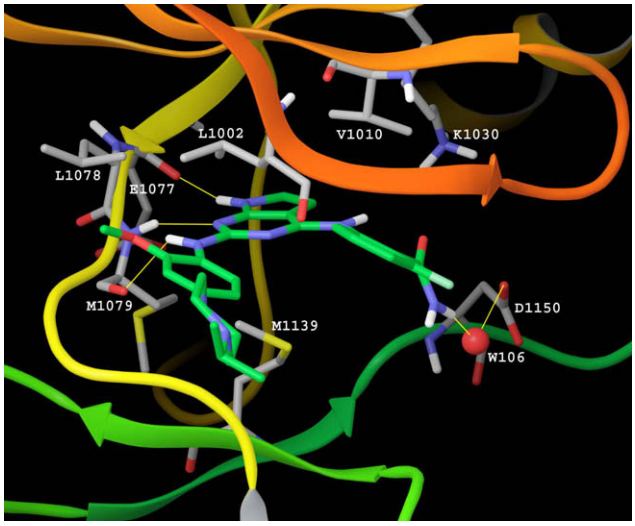

Figure 2. Co-crystal structure of IR Double Mutant (C981S, D1132N, carbon atoms in grey) in complex with **13** (carbon atoms in green). Intermolecular H-bond interactions are highlighted with yellow lines. Crystallographic data for this structure has been deposited at PDB:3EKN.

the C4′ 4-isopropyl-piperazinyl of **13** lay outside the pocket and was solvent exposed.

The loss of IGF-1R activity resulting from alkylation of the hinge-binding motif, as with **14** and **15** (Table 2), is consistent with our crystallographic data and docking model. Direct methylation of the pyrrole moiety (**15**) gave a 5000-fold drop in IGF-1R potency, as expected given the likely disruption of the H-bond interaction between the backbone carbonyl of Glu1050 and the inhibitor deep within the ATP-binding site. For **14**, this was not the case. While substituting a methyl on the C6 amino group would disrupt the H-bond interaction between the backbone carbonyl of Met1052 and the inhibitor, this substitution is adjacent to the protein–solvent interface where a methyl might be accommodated. Given these observations, we expected a loss of enzyme activity for **14** compared to **13**, but not to the extent of that seen with **15**. Indeed, this was the case; the IC_{50} value of **14** against IGF-1R was 50 nM, which was 25-fold lower than the potency of **13** but 200-fold higher than that of **15**.

Table 2
N-methylation at N1 and N7 reduced potency against IGF-1R. (values represent an average of ⩾2 individual measurements)

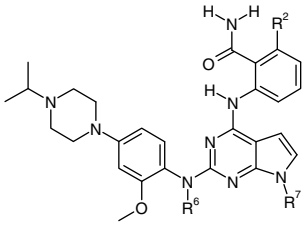

Compound	R^2	R^6	R^7	IGF-1R Enzyme IC_{50} (nm)
13	F	H	H	2
14	F	Me	H	50
15	F	H	Me	10,000

Further structure–activity relationships about the C6 aniline were systematically explored. In the context of an isopropyl piperazine, a variety of substituents were tolerated at C5′ (see **13**, **16**–**19**, Table 3). However, introduction of a 1′,2′,3′,4′-tetrasubstituted aniline via addition of a C3′ substituent (**20** and **21**, Table 2) proved less tolerated, especially in cellular estimates of IGF-1R potency. Interestingly, within the 1′,2′,4′,5′-tetrasubstituted series, reversal of the piperazine and methyl moieties (i.e., **18** vs **23**) gave a logarithmic drop in IGF-1R inhibition at both the enzyme and cellular level. Removal of the methyl substituent at C4′ (**22**) apparently allowed a less constrained disposition of the piperazine ring, and as such perhaps enjoyed a modest improvement in potency relative to **23** as a result of an ionic interaction with Asp 1056.[14] (See Table 4).

In silico predictions[15] with **5** and **24** suggested the C4 carboxamide-containing aniline could pose a metabolic liability, espe-

Table 3
IGF-1R enzyme and phospho IGF-1R cellular IC_{50} results for **13**, **16**–**23**. (values represent an average of ⩾2 individual measurements)

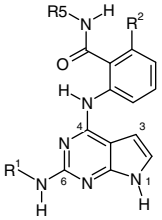

Compound	R^1	X	R^2	IGF-1R enzyme IC_{50} (nM)	Phospho IGF-1R cellular IC_{50} (nM)
13	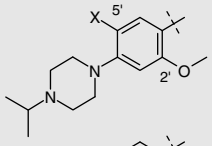	H	–F	2.0	109
16		–OMe	–F	3.2	90
17		–F	–F	2.0	190
18		–Me	–F	2.0	38
19		–Cl	–F	1.6	65
20	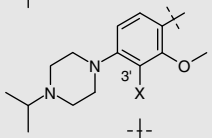	–F	–F	4.0	574
21		–Me	–F	8.0	3700
22	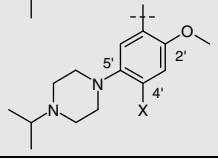	–H	–F	4.0	160
23		–Me	–F	20	270

Table 4
IGF-1R enzyme and phospho IGF-1R cellular IC_{50} results for **11**, **13**, **24–33**. (values represent an average of ⩾2 individual measurements)

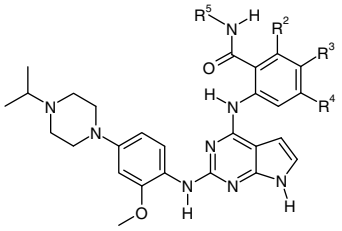

Compound	R^2	R^3	R^4	R^5	IGF-1R Enzyme IC_{50} (nM)	Phospho IGF-1R cellular IC_{50} (nM)
24	H	H	H	–H	1.0	71
13	F	H	H	–H	2.0	109
25	H	F	H	–H	0.8	60
11	H	H	F	–H	0.8	130
26	F	F	H	–H	1.3	213
27	F	H	F	–H	0.8	90
28	H	F	F	–H	0.5	53
29	F	H	H	–Me	5.0	370
30	H	F	H	–Me	3.2	135
31	H	F	H	–OH	6.3	613
32	H	F	H	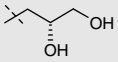	16	5600
33	H	F	H		5.0	650
34	H	F	H	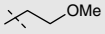	25	760

Table 5
In vivo rat DMPK properties for selected analogs (values represent the average of three animals)

Compound	Dose (mg/kg)		Cl (mL/min/kg)	DNAUC (ng h/mL/mg/kg)	Vss (L/kg)	Cmax (ng/mL)	%F
	IV	PO					
24	1.7	10.5	142	35	19.5	69	37
13	2.1	9.2	51	156	18.5	184	65
27	2.3	10.7	46	117	11.0	200	37
28	4.2	13.6	64	114	17.0	152	45
29	2.0	10.6	32	277	22.3	418	83

cially if unsubstituted at R^2–R^4. As such, it was of interest to systematically explore available fluorine substitutions. A number of combinations of mono- and bis-fluorine substitution (**11**, **13**, **25**–**28**) were well tolerated, giving potencies within 2- to 3-fold of unsubstituted **24**. Modification of the primary carboxamide was in general less tolerated, with small alkyl (**29** and **30**) apparently better accommodated than solubilizing groups exemplified by **31**–**34**.

Consistent with our metabolic predictions, pharmacokinetic measurements made in vivo demonstrated that fluorination about the C(4) aniline proved fruitful in reducing IV clearance (compare **13**, **27**–**28** with **24**, Table 5) in rat. Moreover, simple substitution of the primary carboxamide gave further reduction in IV clearance and overall higher exposure and bioavailability (**29**, Table 5).

In conclusion, a series of 4,6-bis-anilino-1*H*-pyrrolo[2,3-*d*] pyrimidines were demonstrated to be potent inhibitors of the IGF-1R receptor tyrosine kinase. Crystallographic studies of the hinge-binding motif have demonstrated the inhibition of IGF-1R occurs via three-point contact of the pyrrolopyrimidine to the IGF-1R kinase hinge. Modifications of the C6 aniline revealed a C2′ methoxy and C5′ solubilizing group were optimal for inhibition of IGF-1R, while systematic halogenation of the C4 aniline revealed unsubstituted C4 anilines are a key metabolic liability in vivo. A balance of in vitro enzyme and cellular potency[16] and desirable in vivo pharmacokinetic properties make **13** a tool for further investigation of IGF-1R, and its further biological characterization will be reported in due course.

References and notes

1. (a) Mantzoros, C. S.; Tzonou, A.; Signorello, L. B.; Stampfer, M.; Trichopoulos, D.; Adami, H. O. *Br. J. Cancer* **1997**, *769*, 1115; (b) Wolk, A.; Mantzoros, C. S.; Andersson, S. O.; Bergstrom, R.; Signorello, L. B.; Lagiou, P.; Adami, H. O.; Trichopoulos, D. *J. Natl. Cancer Inst.* **1998**, *9012*, 911; (c) Cohen, P. *J. Natl. Cancer Inst.* **1998**, *9012*, 876.
2. Davies, M.; Dupta, S.; Goldspink, G.; Winslet, M. *Int. J. Colorectal Dis.* **2006**, *213*, 201.
3. (a) Papa, V.; Belfiore, A. *J. Endocrinol. Invest.* **1996**, *195*, 324; (b) Papa, V.; Pezzino, V.; Costantino, A.; Belfiore, A.; Giuffrida, D.; Frittitta, L.; Vannelli, G. B.; Brand, R.; Goldfine, I. D.; Vigneri, R. *J. Clin. Invest.* **1990**, *865*, 1503.
4. (a) Moser, C.; Schachtschneider, P.; Lang, S. A.; Gaumann, A.; Mori, A.; Zimmermann, J.; Schlitt, H. J.; Geissler, E. K.; Stoeltzing, O. *Eur. J. Cancer* **2008**, *4411*, 1577; (b) Wolpin, B. M.; Michaud, D. S.; Giovannucci, E. L.; Schernhammer, E. S.; Stampfer, M. J.; Manson, J. E.; Cochrane, B. B.; Rohan, T. E.; Ma, J.; Pollak, M. N.; Fuchs, C. S. *Br. J. Cancer* **2007**, *971*, 98.
5. (a) Sachdev, D.; Yee, D. *Mol. Cancer Ther.* **2007**, *61*, 1; (b) Rodon, J.; DeSantos, V.; Ferry, R.; Kurzrock, R. *Mol. Cancer Ther.* **2008**, *79*, 2575.
6. Lu, Y.; Zi, X.; Zhao, Y.; Mascarenhas, D.; Pollak, M. *N. Natl. Cancer Inst.* **2001**, *9324*, 1852.
7. (a) García-Echeverría, C.; Pearson, M. A.; Marti, A.; Meyer, T.; Mestan, J.; Zimmermann, J.; Gao, J.; Brueggen, J.; Capraro, H. G.; Cozens, R.; Evans, D. B.;

Fabbro, D.; Furet, P.; Porta, D. G.; Liebetanz, J.; Martiny-Baron, G.; Ruetz, S.; Hofmann, F. *Cancer Cell* **2004**, *53*, 231; (b) Mulvihill, M. J.; Ji, Q. S.; Coate, H. R.; Cooke, A.; Dong, H.; Feng, L.; Foreman, K.; Rosenfeld-Franklin, M.; Honda, A.; Mak, G.; Mulvihill, K. M.; Nigro, A. I.; O'Connor, M.; Pirri, t C.; Steinig, A. G.; Siu, K.; Stolz, K. M.; Sun, Y.; Tavares, P. A.; Yao, Y.; Gibson, N. W. *Bioorg. Med. Chem.* **2008**, *163*, 1359; (c) Ji, Q. S.; Mulvihil, l M. J.; Rosenfeld-Franklin, M.; Cooke, A.; Feng, L.; Mak, G.; O'Connor, M.; Yao, Y.; Pirritt, C.; Buck, E.; Eyzaguirre, A.; Arnold, L. D.; Gibson, N. W.; Pachter, J. A. *Mol. Cancer Ther.* **2007**, *68*, 2158; (d) Mulvihill, M. J.; Ji, Q. S.; Werner, D.; Beck, P.; Cesario, C.; Cooke, A.; Cox, M.; Crew, A.; Dong, H.; Feng, L.; Foreman, K. W.; Mak, G.; Nigro, A.; O'Connor, M.; Saroglou, L.; Stolz, K. M.; Sujka, I.; Volk, B.; Weng, Q.; Wilkes, R. *Bioorg. Med. Chem. Lett.* **2007**, *174*, 1091; (e) Saulnier, M. G.; Frennesson, D. B.; Wittman, M. D.; Zimmermann, K.; Velaparthi, U.; Langley, D. R.; Struzynski, C.; Sang, X.; Carboni, J.; Li, A.; Greer, A.; Yang, Z.; Balimane, P.; Gottardis, M.; Attar, R.; Vyas, D. *Bioorg. Med. Chem. Lett.* **2008**, *185*, 1702; (f) Velaparthi, U.; Liu, P.; Balasubramanian, B.; Carboni, J.; Attar, R.; Gottardis, M.; Li, A.; Greer, A.; Zoeckler, M.; Wittman, M. D.; Vyas, D. *Bioorg. Med. Chem. Lett.* **2007**, *1711*, 3072; (g) Velaparthi, U.; Wittman, M.; Liu, P.; Stoffan, K.; Zimmermann, K.; Sang, X.; Carboni, J.; Li, A.; Attar, R.; Gottardis, M.; Greer, A.; Chang, C. Y.; Jacobsen, B. L.; Sack, J. S.; Sun, Y.; Langley, D. R.; Balasubramanian, B.; Vyas, D. *Bioorg. Med. Chem. Lett.* **2007**, *178*, 2317; (h) Bell, I. M.; Stirdivant, S. M.; Ahern, J.; Culberson, J. C.; Darke, P. L.; Dinsmore, C. J.; Drakas, R. A.; Gallicchio, S. N.; Graham, S. L.; Heimbrook, D. C.; Hall, D. L.; Hua, J.; Kett, N. R.; Kim, A. S.; Kornienko, M.; Kuo, L. C.; Munshi, S. K.; Quigley, A. G.; Reid, J. C.; Trotter, B. W.; Waxman, L. H.; Williams, T. M.; Zartman, C. B. *Biochemistry* **2005**, *4427*, 9430.

8. Chamberlain, S.; Lei, H.; Moorthy, G.; Patnaik, S.; Gerding, R.; Redman, A.; Stevens, K.; Wilson, J.; Yang, B.; Shotwell, *J. Org. Chem.* **2008**, in press. doi: 10.1021/jo8020693.
9. (a) Autsch, A.; Zoephel, A.; Ahorn, H.; Spevak, W.; Hauptmann, R.; Nar, H. *Structure* **2001**, *9*, 955. PDB: 1JQH; (b) Favelyukis, S.; Till, J.; Hubbard, S.; Miller, W. *Nat. Struct. Biol.* **2001**, *8*, 1058. PDB 1K3A; (c) Munshi, S.; Kornienko, M.; Hall, D.; Reid, J.; Waxman, L.; Stirdivant, S.; Darke, P.; Kuo, L. *J. Biol. Chem.* **2002**, *277*, 38797. PDB 1M7N.
10. IGF-1R enzyme assay: GST-rTEV-IGF-1R(957-1367) containing amino acid residues 957–1367 was purified from a baculovirus expression system in *Sf9* cells using Glutathione Sepharose 4FF column chromatography followed by Sephadex-200 size exclusion column chromatography. Assays were performed in 384-well (Greiner, Catalog No. 784076) microtiter plates. Reaction buffer (50 mM HEPES buffer, pH 7.5; 10 mM $MgCl_2$; 3 mM DTT; 1 mM CHAPS; 0.1 mg/ml BSA) for peptide phosphorylation (10 μl volume) contained, in final concentrations, 500 nM biotinylated peptide substrate; 10 μM ATP; and purified, activated hIGF-1R or hIR (0.5 nM). Activation of GST-rTEV-IGF-1R(957-1367) was achieved by a 4 min incubation of hIGF-1R (2.7 μM final) with 2 mM ATP in 50 mM HEPES, 20 mM $MgCl_2$, 0.1 mg/ml BSA, at room temperature. Compounds, titrated in DMSO, were evaluated at eleven concentrations ranging from 50 μM to 0.2 nM. Reactions were incubated for 1 h at room temperature and were stopped by a 5 μl addition of EDTA (to 33 mM). A further addition of 5 μl detection reagents (for final 7 nM Streptavidin-APC (Perkin-Elmer #CR130-150), 1 nM Europium-labeled anti-phosphotyrosine monoclonal antibody (Perkin-Elmer #AD0067), added in reaction buffer (without DTT), was required for signal generation. After 30 min, signal was read on Perkin-Elmer Viewlux microplate imager or Wallac Victor fluorometer.
11. Phospho IGF-1R Cellular Assay: NIH-3T3 cells overexpressing human IGF-1R were plated in 96-well plates (10,000 cells/well) in culture media containing 10% fetal bovine serum and incubated at 37 °C in a 5% CO_2 incubator. Twenty four hours post-plating, cells were treated with different concentrations of test compounds ranging from 30 μM to 1.5 nM. 2 h after compound addition, cells were stimulated with human IGF-1 (30 ng/ml). Cell lysates were analyzed for phosphorylated receptors using dissociation enhanced lanthanide fluor-immuno assay (DELFIA) with anti-IGF-1R (MAB391, R&D Systems, Minneapolis, MN) capture antibody and europium-labeled anti-pTyr antibody (Eu-N1 PT66, Perkin-Elmer, Waltham, MA) for detection. The fluorescence signal for cells treated with compounds was expressed as percent relative to 100% stimulation (IGF-1 stimulated signal). Concentration of test compound that inhibited 50% of ligand-induced receptor phosphorylation (IC_{50}) was determined by 4 parameter fit of data using XLfit, (value of no cell control was subtracted from all samples for background).
12. The methoxy-substitution on the C6 aniline afforded a large selectivity over Aurora B kinase as measured in vitro. IC_{50}s against Aurora B for **2**, **3**, and **5** were estimated as 5 nM, 1600 nM, and >10,000 nM, respectively. This is consistent with known binding pocket differences between Aurora B and IGF-1R.
13. Castagnoli, N.; Rimoldi, J.; Bloomquist, J.; Castagnoli, K. *Chem. Res. Toxicol.* **1997**, *10*, 924.
14. Direct targeting of C6 aniline substituents toward Asp1056 is the topic of the accompanying paper.
15. Cruciani, G.; Carosati, E.; De Boeck, B.; Ethirajulu, K.; Mackie, C.; Howe, T.; Vianello, R. *J. Med. Chem.* **2005**, *4822*, 6970.
16. Estimates of the impact of plasma protein binding on overall potency for **13** and **29** could be made by carrying out the phospho IGF-1R cellular assay (see Ref. 11) in the presence of 2% HAS and 0.1% AAG. Under these conditions, reductions in observed IC_{50} values for **13** and **29** were observed to be only 1.7- and 1.6-fold, respectively.